ACCOUNTS of chemical research

Article

pubs.acs.org/accounts

Synthesis of Two-Dimensional Materials by Selective Extraction

Published as part of the Accounts of Chemical Research special issue "2D Nanomaterials beyond Graphene".

Michael Naguib[†] and Yury Gogotsi*[,‡]

[†]Materials Science and Technology Division, Oak Ridge National Laboratory, Oak Ridge, Tennessee 37381, United States

[‡]Department of Materials Science and Engineering and A. J. Drexel Nanomaterials Institute, Drexel University, Philadelphia, Pennsylvania 19104, United States

CONSPECTUS: Two-dimensional (2D) materials have attracted much attention in the past decade. They offer high specific surface area, as well as electronic structure and properties that differ from their bulk counterparts due to the low dimensionality. Graphene is the best known and the most studied 2D material, but metal oxides and hydroxides (including clays), dichalcogenides, boron nitride (BN), and other materials that are one or several atoms thick are receiving increasing attention. They may deliver a combination of properties that cannot be provided by other materials.

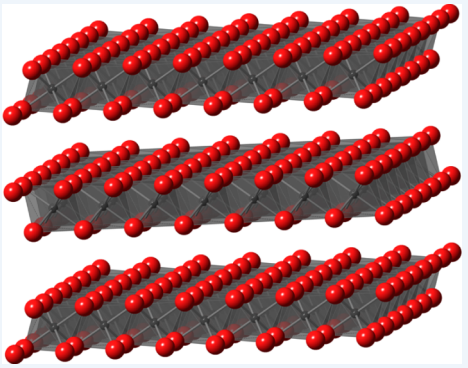

The most common synthesis approach in general is by reacting different elements or compounds to form a new compound. However, this approach does not necessarily work well for low-dimensional structures, since it favors formation of energetically preferred 3D (bulk) solids. Many 2D materials are produced by exfoliation of van der Waals solids, such as graphite or MoS_2, breaking large particles into 2D layers. However, these approaches are not universal; for example, 2D transition metal carbides cannot be produced by any of them. An alternative but less studied way of material synthesis is the selective extraction process, which is based on the difference in reactivity and stability between the different components (elements or structural units) of the original material. It can be achieved using thermal, chemical, or electrochemical processes. Many 2D materials have been synthesized using selective extraction, such as graphene from SiC, transition metal oxides (TMO) from layered 3D salts, and transition metal carbides or carbonitrides (MXenes) from MAX phases.

Selective extraction synthesis is critically important when the bonds between the building blocks of the material are too strong (e.g., in carbides) to be broken mechanically in order to form nanostructures. Unlike extractive metallurgy, where the extracted metal is the goal of the process, selective extraction of one or more elements from the precursor materials releases 2D structures. In this Account, in addition to graphene and TMO, we focused on MXenes as an example for the use of selective extraction synthesis to produce novel 2D materials. About 10 new carbides and carbonitrides of transition metals have been produced by this method in the past 3 years. They offer an unusual combination of metallic conductivity and hydrophilicity and show very attractive electrochemical properties. We hope that this Account will encourage researchers to extend the use of selective extraction to other layered material systems that in turn will result in expanding the world of nanomaterials in general and 2D materials in particular, generating new materials that cannot be produced by other means.

■ INTRODUCTION

Usually, new chemical compounds or materials are produced by combining elements or compounds through chemical reactions, forming new chemical bonds and new structures. However, there are many cases known when selective corrosion, dissolution, or oxidation lead to formation of new structures. For example, dealloying one metal, such as copper, from its alloys, (Cu−Au[1] or Cu−Pt[2]) results in nanoporous metals. Similarly, etching metals from metal carbides results in forming carbide derived carbon (CDC), with a high specific surface area and a tunable pore size.[3] The concept of selective extraction synthesis is simply based on the difference in reactivity of different elements in the compound under certain conditions, which allows some of the elements to leave the material producing unique nanostructures. It is worth noting that the different reactivity is not necessarily a result of different elemental composition, but it can be due to allotropic modifications or defects in the crystal structure, such as stacking faults in cubic (3C)-β-SiC whiskers.[4] This difference in reactivity resulted in an anisotropic etching in a mixture of hydrofluoric and nitric acids producing few-nanometer thick flakes and pagoda-like SiC nanostructures.[4]

New two-dimensional (2D) materials such as transition metal carbides and carbonitrides, so-called MXenes,[5] were synthesized from their strongly bonded 3D layered counterparts by selective extraction. Herein we review the synthesis of 2D materials by selective extraction. The 2D materials covered

Special Issue: 2D Nanomaterials beyond Graphene

Received: September 20, 2014
Published: December 9, 2014

DOI: 10.1021/ar500346b
Acc. Chem. Res. 2015, 48, 128−135

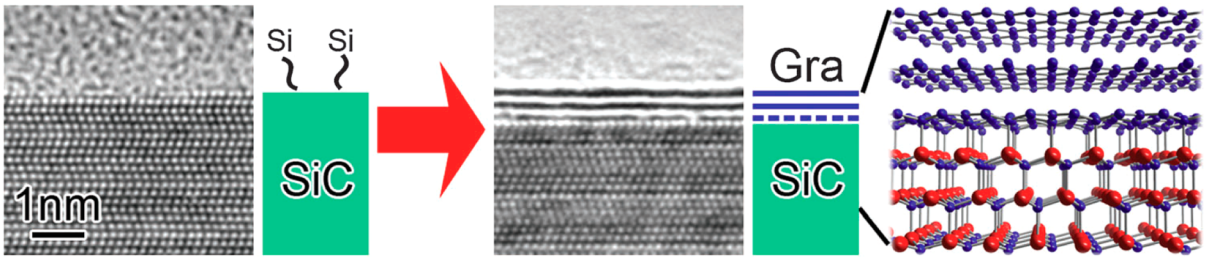

Figure 1. Transmission electron micrographs and a schematic of the synthesis of graphene from SiC by sublimating Si from the structure. The red atoms represent silicon, while blue atoms represent carbon. Reproduced with permission from ref 9. Copyright 2014 Royal Society of Chemistry.

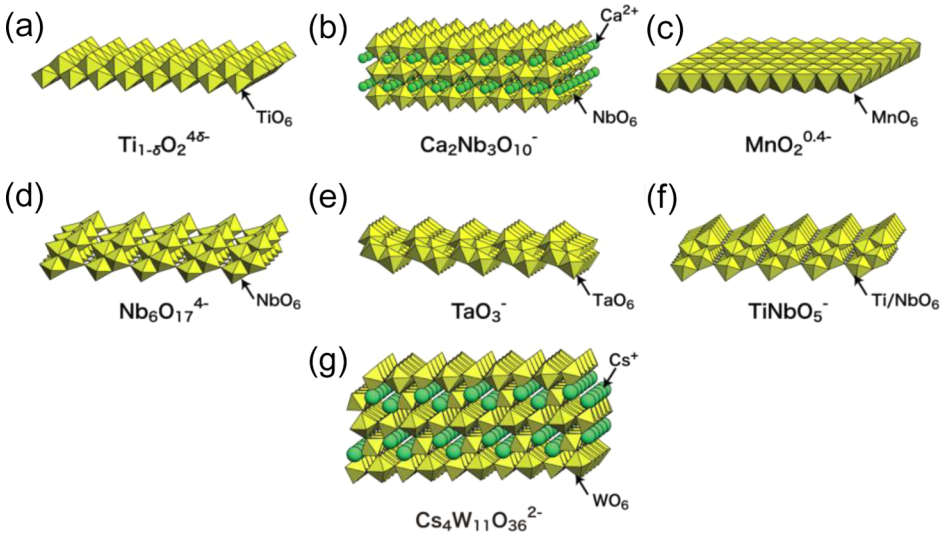

Figure 2. Schematic of the structure of 2D oxides of (a) titanium, (b) calcium−niobium, (c) manganese, (d) niobium, (e) tantalum, (f) titanium−niobium, and (g) cesium−tungsten. Reproduced with permission from ref 21. Copyright 2010 Wiley-VCH Verlag GmbH: Advanced Materials.

include graphene, transition metal oxides, and transition metal carbides and nitrides (MXenes).

GRAPHENE

Heating single crystals of silicon carbide, SiC, under high vacuum (~10^{-6} Torr)[6] or under argon[7] produces epitaxial graphene. Due to the high vapor pressure of Si compared with C,[8] Si sublimes from the surface during heating and leaves behind a C-rich surface. Then the carbon rich surface graphitizes forming graphene. Formation of a single graphene layer requires decomposition of three layers of SiC.[6] A schematic for the process is shown in Figure 1.[9] This technique was first reported by Van Bommel et al.[6] in 1975. It is worth noting that, in parallel to the early work by Novoselov et al.,[10] Berger et al.[11] used SiC to produce few-layer graphene, and they explored graphene's electronic properties, but their paper was published about 6 weeks after ref 10.

The surface termination of the SiC single crystal affects the number of graphene layers; in the case of the Si-face that corresponds to (0001), homogeneous few-layer graphene is formed; while in case of C-face corresponding to $(000\bar{1})$, more disordered multilayer graphene is formed. Unique rotational disorder of the graphene layers was observed in case of C termination.[12] It is worth noting that changing the synthesis temperature or vacuum pressure may result in formation of other forms of carbon such as carbon nanotubes and graphite.[13] Heating rate was found to play an important role in the synthesis process, especially considering the surface steps on SiC, faster heating leads to larger single-layer graphene areas.[14]

One of the advantages of using this technique is the ability to control the number of graphene layers by controlling the synthesis temperature and time.[15] More importantly, the graphene produced using this technique can be used on the SiC wafer as is, with no need for transferring to other substrates. This makes graphene, produced by the selective extraction of Si from SiC, promising for wafer-scale electronics applications.[16] A detailed review dedicated mainly to the graphene produced by this method can be found in ref 9. It is important to mention that 2D but less ordered CDC can be produced by extracting metals from other carbides chemically[3] or electrochemically.[17]

LAYERED TRANSITION METAL OXIDES

Two-dimensional transition metal oxides (TMO) have attractive properties, and they are promising for many applications varying from electronics[18] to electrochemical energy storage.[19,20] In layered TMOs (Figure 2), each layer is a negatively charged slab of corner- or edge-shared octahedral units of MO_6 (M is Ti, Nb, Mn, W, etc.) with alkali cations (K^+, Cs^+, etc.) filling the interlayer spacing.[21] Unlike graphene and transition metal dichalcogenides (TMDs), the negatively charged layers here are ionically bonded together through the alkali cations.[21] Thus, selective extraction is usually needed to exfoliate these layered oxides, which involves selective leaching of the alkali cations.[18] Layered vanadium (V_2O_5) and molybdenum (MoO_3) oxides can be considered exceptions, because of weak van der Waals bonds between the layers, so no leaching is needed to produce 2D layers of them.[20,22]

DOI: 10.1021/ar500346b
Acc. Chem. Res. 2015, 48, 128−135

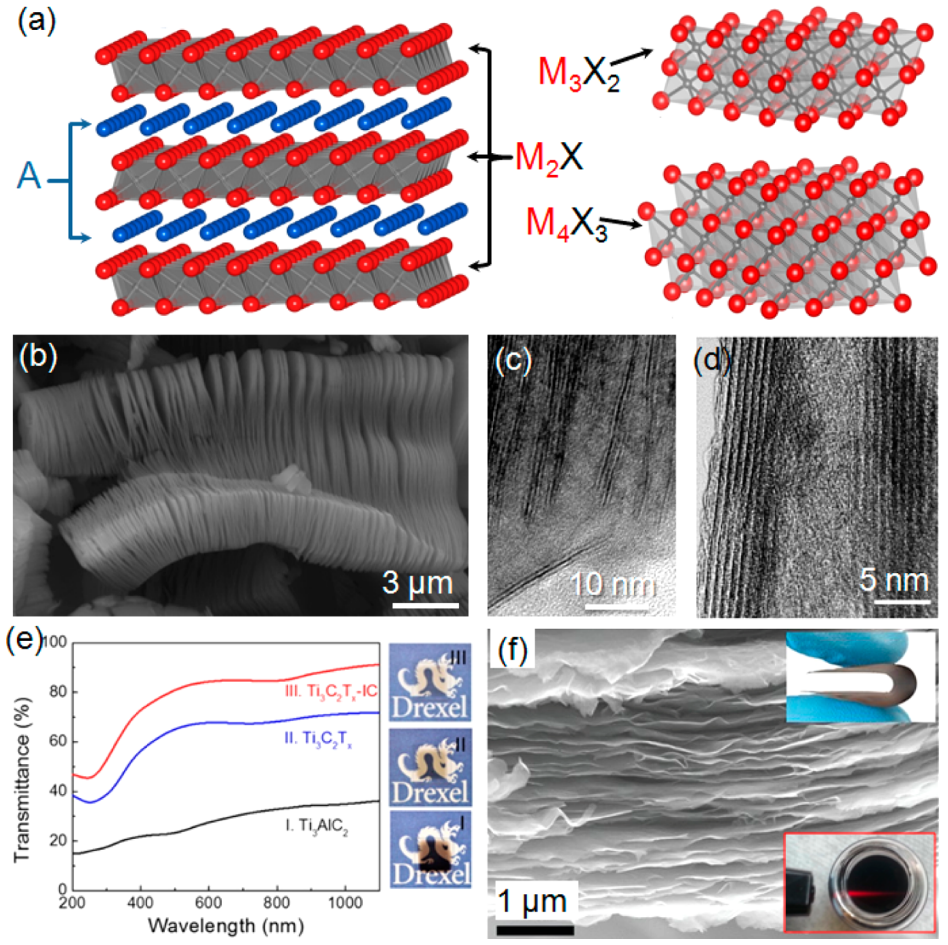

Figure 3. (a) Schematics of the M_2AX crystal structure and M_3X_2 and M_4X_3 layers. (b) SEM image of $Ti_3C_2T_x$.[42] (c, d) Cross-sectional TEM images of Nb_2CT_x sheets and $Ti_3C_2T_x$ scroll, respectively.[41] (e) Transmittance vs wavelength for epitaxial thin films of (I) Ti_3AlC_2, (II) $Ti_3C_2T_x$, and (III) $Ti_3C_2T_x$ intercalated with NH_3 and NH_4^+. Optical images of the films are shown at the right side of the graph.[50] (f) SEM image of $Ti_3C_2T_x$ paper made by filtering a colloidal suspension of delaminated MXene. The lower inset is an optical image of the colloidal suspension of delaminated $Ti_3C_2T_x$ in water with laser pointer showing the Tyndal effect; the upper inset shows an optical image of the paper bent between the fingers without breakage.[56] Panel b was reproduced with permission from ref 42. Copyright 2012 American Chemical Society. Panel c was reproduced with permission from ref 41. Copyright 2013 American Chemical Society. Panel d was reproduced with permission from ref 35. Copyright 2011 WILEY-VCH Verlag GmbH: Advanced Materials. Panel e was reproduced with permission from ref 50. Copyright 2014 American Chemical Society. Panel f was reproduced with permission from ref 56. Copyright 2013 AAAS/Science.

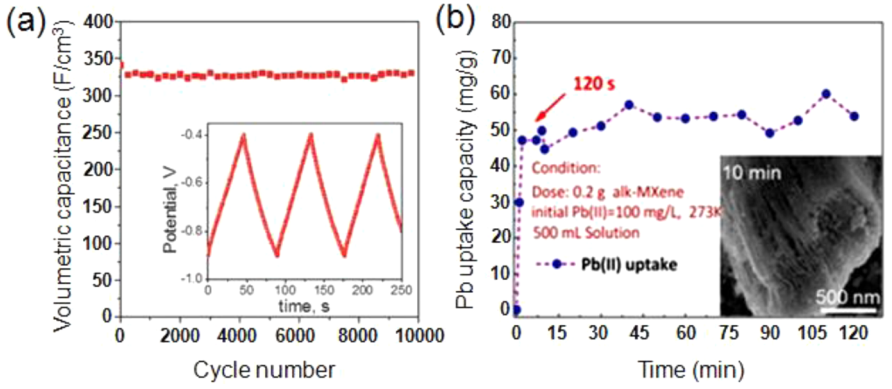

Figure 4. (a) Volumetric capacitance vs cycle number for $Ti_3C_2T_x$ paper electrode in electrochemical capacitor with 1 M KOH electrolyte and cycled at 1 A/g. The inset shows the galvanostatic cycling results from which the cyclability figure was plotted.[56] (b) Lead uptake capacity of alkalized $Ti_3C_2T_x$ vs time. The inset shows SEM image of a MXene particle after 10 min in Pb containing water.[87] Panel a was reproduced with permission from ref 56. Copyright 2013 AAAS/Science. Panel b was reproduced with permission from ref 87. Copyright 2014 American Chemical Society.

The reaction between layered TMO and aqueous acids, for example, HCl, results in the etching of the alkali cations from between the layers and their replacement with protons.[21,23−25] Sugahara et al.[26,27] reported that protonated layered perovskite

DOI: 10.1021/ar500346b
Acc. Chem. Res. 2015, 48, 128−135

can be also produced by selective etching of bismuth oxide sheets from Aurivillius phases. The protonated TMO layers can be considered as a solid acid that has a high affinity for bases.[23] Therefore, immersing the protonated TMO in organic base, such as tetrabutylammonium (TBA) hydroxide, results in exchanging the protons with organic cations, for example, TBA^+, accompanied by a drastic increase in the interlayer spacing.[18,28] Then, TMOs are delaminated by mild sonication[29] or simply by shaking,[30] forming colloidal solutions of 2D layers. The use of tetramethylammonium (TMA) instead of TBA resulted in 2D layers of TMO with larger lateral size.[31] The larger size of TBA results in larger mechanical stress and, in turn, fragmentation of the TMO layers into pieces.[31] For more details about 2D layers of TMO, we refer the readers to comprehensive reviews by Sasaki et al.[18,21]

TRANSITION METAL CARBIDES AND CARBONITRIDES (MXENES)

Transition metal carbides and nitrides (TMC/Ns) possess high electrical and thermal conductivities, good mechanical properties, and chemical stability.[32,33] Most of the TMC/Ns have the rock-salt structure, but some have a hexagonal structure (e.g., V_2C).[34] In all cases, strong bonding (mixture of metallic, covalent, and ionic) is common, and 2D TMC/Ns were not known before 2011.[35] However, TMC/N layers separated by other atoms exist in a large family (>70 members) of layered ternary compounds with hexagonal structure ($P6_3/mmc$), called MAX phases.[36] They have a general formula of $M_{n+1}AX_n$, where "M" is an early TM (Ti, Nb, Mo, etc.), "A" is a group A element (Al, Si, Sn, etc.), "X" is carbon or nitrogen or both, and $n = 1-3$.[36] Mn containing MAX phases were synthesized recently.[37] Also, solid solutions on the M site, such as $(Ti_{0.5}Nb_{0.5})_2AlC$, and on the A site, such as $Ti_3(AlSi)C_2$, exist, in addition to carbonitrides, such as Ti_3AlCN.

Figure 5. (a) Schematic for the oxidation of Ti_3C_2 forming nanotitania on thin sheets of carbon. Reproduced with permission from ref 88. Copyright 2014 Royal Society of Chemistry.

As shown in Figure 3a, the crystal structure of MAX phases can be described as layers of edge shared M_6X octahedrons intercalated with pure A-group element layers. Depending on the n value, the thickness of the $M_{n+1}X_n$ changes; if $n = 1$, then the layer consists of a single block of octahedra, if $n = 2$, two blocks, and if $n = 3$, three blocks of octahedra. Also, hybrid crystals of MAX phases were reported, such as $Ti_5Al_2C_3$, which is a mixture of Ti_2AlC and Ti_3AlC_2.[38] Similar to TMC, the bonds between the M and X are covalent−ionic, while those between M and A are metallic making mechanical exfoliation reported for graphite, boron nitride, and TMDs[39] difficult. Zhang et al.[40] reported on the exfoliation of $Ti_3(Si_{0.75}Al_{0.25})C_2$ by sonication in various solvents. The solid solution of Si−Al in the A layer weakened the bonds and facilitated the exfoliation process, because the same treatment on Ti_3SiC_2 did not result in any exfoliation.[40]

In most MAX phases, the A layer is more reactive than the $M_{n+1}X_n$ layers. Taking advantage of the difference in reactivity, the A layers were selectively etched from MAX phases in aqueous hydrofluoric acid (HF) at room temperature leaving stacks of $M_{n+1}X_n$ 2D layers.[5,35,41−43] As a result of etching the A layers, the M atoms on the outer surface are terminated with functional groups (OH, O, or F), referred to as T_x, and metallic bonds between $M_{n+1}X_n$ layers through the A atoms were replaced by weak bonds between surface functional groups. Sonicating the $M_{n+1}X_nT_x$ stacks resulted in separation of 2D layers. We named them "MXenes" as derivatives from MAX phases but without the A atoms with the suffix "ene" to emphasize their dimensionality analogous to graphene. Figure 3b shows a typical scanning electron microscopy (SEM) image for a stack of MXenes, while Figure 3c shows a cross-sectional TEM image of MXene sheets after sonication. So far, the following MXenes have been reported experimentally: $Ti_3C_2T_x$,[35,44] Nb_2CT_x, V_2CT_x,[41] Ti_2CT_x, $(Ti_{0.5}Nb_{0.5})_2CT_x$, $(V_{0.5}Cr_{0.5})_3C_2T_x$, $Ta_4C_3T_x$, Ti_3CNT_x,[42] and $Nb_4C_3T_x$.[43] Many more are expected to be stable.[45,46]

While all the MXenes reported to date were synthesized from their aluminum-containing MAX phase counterparts, the etching conditions varied significantly.[5] For example, to etch Al from Ti_2AlC in order to produce Ti_2CT_x, 10% HF for 10 h at RT was sufficient,[42] while in the case of Nb_2AlC, 50% HF for 90 h at RT was needed.[41] This can be explained by the different bond energies between the outer M atoms in the $M_{n+1}X_n$ and the A atoms; for example, the bond energy of Nb−Al is higher than that of Ti−Al.[47] The etching time can be reduced significantly by decreasing the particle size or increasing the temperature slightly (<65 °C).[48] Excessive heating may result in complete dissolution of carbide[42] or recrystallization of the MXene layers.[49] For example, hydrothermal treatment of

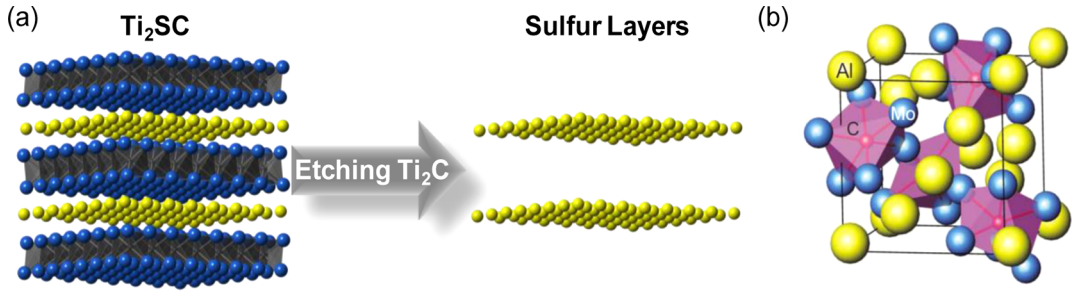

Figure 6. Schematics of (a) sulfur layer formation upon etching the Ti_2C blocks from the Ti_2SC [blue spheres, Ti atoms, and black, C atoms in the center of the octahedrons, while yellow spheres represent S atoms] and (b) crystal structure of Mo_3Al_2C. Panel b was reproduced with permission from ref 89. Copyright 2010 American Physical Society.

DOI: 10.1021/ar500346b
Acc. Chem. Res. 2015, 48, 128−135

Ti_3AlC_2 at 180 °C for 1 h in HF solution etched the Al, but the Ti_3C_2 layers formed titanium carbide with rock-salt structure.[49]

Etchants other than HF have been explored. Halim et al.[50] reported using aqueous 1 M ammonium bifluoride (NH_4HF_2) as an etchant at RT, which resulted in conversion of Ti_3AlC_2 into Ti_3CT_x intercalated with NH_3 and NH_4^+ during the reaction. HF formed *in situ* by reaction of fluorides (e.g., LiF) with HCl can also etch MAX phases forming MXenes.[51] This completely eliminates the use of HF as a starting reagent but still does not eliminate fluorine from the system. Xie et al.[52] attempted to use a fluoride-free reaction by treating Ti_3AlC_2 with aqueous 1 M NaOH for 100 h at 80 °C followed by hydrothermal treatment in 1 M H_2SO_4 at 80 °C for 2 h, but Al was etched only from the outer surface of the MAX phase. Clearly, more efforts are still needed to develop a fluoride-free synthesis procedure of MXenes.

The as-synthesized MXenes have a morphology very similar to exfoliated graphite (Figure 3b);[53] also their electric resistivities are comparable to multilayer graphene.[42] Similar to graphene, some of the MXene sheets scroll up during sonication (Figure 3d).[35] In addition to being electronically conductive, MXenes are hydrophilic.[42] This combination of hydrophilicity with good electrical conductivity is rare in 2D materials. Intercalated epitaxial films of MXenes with thickness around 19 nm transmit about 90% of light in the visible-to-infrared range (Figure 3e).[50] Intense surface plasmons were found for $Ti_3C_2T_x$ at low energies (~0.3 eV).[54]

Many compounds were found to intercalate chemically, spontaneously, between the MXene layers, including hydrazine, polar organic molecules, such as urea and dimethyl sulfoxide (DMSO),[55] and cations.[56] This intercalation ability was explained by the weak coupling/interaction between the MXenes layers,[54] and the negative surface charge of MXenes. The intercalation increases the *c* lattice parameter (LP) of MXenes,[55−57] but for some cations, a decrease in the *a* LP was also observed.[58] Intercalation of DMSO between the layers of $Ti_3C_2T_x$ was accompanied by co-intercalation of water that resulted in a significant increase in the interlayer spacing, so sonicating DMSO-intercalated MXene in water resulted in delamination of the MXene layers forming a stable colloidal solution (bottom right side inset of Figure 3f).[55] The majority of 1 nm-thick MXene flakes in the colloidal solution have lateral size of around half a micrometer, while some flakes have a lateral size of few micrometers.[55] The surface of the as synthesized $Ti_3C_2T_x$ flakes in water is negatively charged with a ζ-potential of about −40 mV.[59] As shown in Figure 3d, filtering this suspension resulted in a flexible MXene paper. The latter showed excellent performance as an electrode for Li-ion batteries (LIBs)[55] and electrochemical capacitors.[56] It was found experimentally that intercalation changes the electronic and optical properties of MXenes,[50,55] showing a potential for sensor applications and coatings with electrochemically tunable color or transparency.

Modeling and simulation, including density functional theory (DFT), were used extensively to understand MXene structure, to predict properties, and to identify applications.[45,46,60−80] For example, MXenes are expected to be quite stiff with in-plane elastic constants from 512 to 788 GPa, depending on the composition.[71] Ti_2C MXene is expected to be less stiff than graphene and h-BN but comparable to MoS_2.[65] The MXenes' band gaps are expected to be between 0 and 2 eV. The electronic properties range from metallic to semiconducting depending on the surface termination.[35,45] The latter is not limited to O, OH, and F, but also methoxy and other terminations are expected to be stable.[74] Semiconductor MXenes are expected to have very high Seebeck coefficients at low temperatures (1140 μV/K at 100 K for Ti_2CO_2), suggesting thermoelectric applications are possible.[45] Cr_2CT_x and Cr_2NT_x are predicted to be ferromagnetic,[45] and the magnetic moments of MXenes can be tuned by exerting mechanical strain.[73] Also, strain is predicted to result in a change from indirect to direct band gap in Sc_2CO_2.[72]

Relatively few of the potential applications of MXenes have been explored. Due to their electrical conductivity and intercalation ability, MXenes showed promising performance as electrodes for LIBs with an excellent rate handling capability,[41,55,81] which was explained by a low Li diffusion barrier on the surface of MXenes.[77,79] Also, it is expected that the diffusion barrier would not be affected by the Li concentration or strain, and mechanical properties of Ti_2C MXenes would not be affected by the Li adsorption.[80] Most of the work was done on the as-synthesized MXenes without control of the surface chemistry, which is expected to play a pivotal role in enhancing MXenes' performance.[77,79] In addition to LIBs, MXenes showed, experimentally, promise in Na-ion and K-ion batteries[78] and are predicted to have high capacity for multivalent ions such as Ca^{2+},[67,78] Mg^{2+}, and Al^{3+}.[78] MXenes are also expected to show high hydrogen uptake,[68,69] for example, 9 wt % in Sc_2C.[69]

Ti_2CT_x MXene was used as a Li-ion hosting electrode in asymmetric Li-ion capacitors and exhibited an energy density of 30 Wh/kg at a power density of 930 W/kg for 1000 cycles.[57] An outstanding volumetric capacitance exceeding 330 F/cm^3, which did not change after 10 000 cycles (Figure 4a), was achieved when $Ti_3C_2T_x$ MXene was used as an electrode material for electrochemical capacitors in KOH electrolyte.[56] This high capacitance was explained by the cation intercalation between the MXene layers.[56,82] Values up to 900 F/cm^3 were reported using H_2SO_4 electrolyte.[51,83]

MXenes' morphology, composition, and stability make them attractive as supports for catalysts including Ru,[84] Cu_2O,[85] and Pt in fuel cells and in oxygen reduction reactions.[52,86] $Ti_3C_2T_x$ treated with NaOH showed selective and fast Pb(II) adsorption (140 mg/g); equilibrium was achieved within 2 min (Figure 4b), which is faster than most other materials.[87] This suggests MXenes also have potential for water purification.

Oxidation of MXenes results in formation of a TMO on atomically thin carbon (Figure 5)[88] by the reaction: $Ti_3C_2O_2 + 2O_2 = 3TiO_2 + 2C$. These hybrids can be used for electrochemical energy storage applications including LIBs and pseudocapacitors.

Extending the extractive synthesis approach to other materials may lead to many novel nanostructures. For example, as shown in Figure 6a, selective dissolution of titanium and carbon from layered Ti_2SC could result in 2D layers of sulfur. Similarly, 2D layers of Si could be synthesized from Ti_3SiC_2. Selective etching of metal from ternary carbides is not limited to 2D structures and can be extended to materials other than MAX phases to produce porous networks and unique nanostructures. Etching Al from cubic Mo_3Al_2C (Figure 6b)[89] could potentially form a highly porous network of Mo_6C clusters, which could be promising as a catalyst.

CONCLUSIONS

Many 2D materials, including carbons, oxides, carbides, and nitrides, can be produced using selective extraction synthesis.

DOI: 10.1021/ar500346b
Acc. Chem. Res. 2015, 48, 128−135

This is a powerful approach that led not only to graphene, the most studied material nowadays, but also to a new family of 2D carbides and nitrides. We envision its application to other material systems in the future. Large area graphene sheets were synthesized from SiC by sublimating Si at high temperatures. Two-dimensional TMOs were produced from their layered 3D counterparts by selective etching of the alkali cations followed by protonation of the surfaces, then exchange of the protons with large organic molecules. After that, the intercalated TMO can be delaminated, forming a colloidal solution. Selective etching of Al from MAX phases at room temperature resulted in 2D layers of TMCs called MXenes. Molecules and ions can intercalate between the MXene layers. MXenes showed promise as electrodes for electrochemical capacitors and LIBs, catalyst supports, selective sorbents, and other applications. Also, MXenes can be used as precursors for hybrid structures of 2D carbon decorated with nanoparticles of TMOs.

AUTHOR INFORMATION

Corresponding Author

*E-mail: Gogotsi@drexel.edu.

Funding

M.N. was sponsored by the Laboratory Directed Research and Development Program of Oak Ridge National Laboratory, managed by UT-Battelle, LLC, for the U.S. Department of Energy. Y.G. was supported by the Fluid Interface Reactions, Structures and Transport (FIRST) Center, an Energy Frontier Research Center funded by the U.S. Department of Energy, Office of Science, and Office of Basic Energy Sciences.

Notes

The authors declare no competing financial interest.

Biographies

Dr. Michael Naguib is a Wigner Fellow at Oak Ridge National Laboratory. He obtained his Ph.D. in Materials Science and Engineering from Drexel University, Philadelphia, PA, USA. He received his M.S. and B.S. degrees in Metallurgical Engineering from the Faculty of Engineering, Cairo University, Egypt. His research focuses on the synthesis and characterization of functional nanomaterials for energy storage. He has published 27 papers in international journals and is a co-inventor on the MXene patent. He has received many international awards, such as MRS Gold Graduate Student Award, Graduate Excellence in Materials Science (GEMS) Award, and Ross Coffin Purdy Award.

Prof. Yury Gogotsi is Distinguished University Professor and Trustee Chair of Materials Science and Engineering at Drexel University. He also serves as Director of the A.J. Drexel Nanomaterials Institute. His Ph.D. is in Physical Chemistry from Kiev Polytechnic and D.Sc. in Materials Engineering from Ukrainian Academy of Sciences. He works on nanostructured carbons and other nanomaterials for energy, water, and medicine. He has coauthored more than 400 journal papers and obtained more than 50 patents. He has received numerous national and international awards for his research and was elected a Fellow of AAAS, MRS, ECS, and ACerS and a member of the World Academy of Ceramics.

REFERENCES

(1) Ding, Y.; Kim, Y. J.; Erlebacher, J. Nanoporous Gold Leaf: "Ancient Technology"/Advanced Material. *Adv. Mater.* **2004**, *16*, 1897−1900.

(2) Pugh, D. V.; Dursun, A.; Corcoran, S. G. Formation of Nanoporous Platinum by Selective Dissolution of Cu from $Cu_{0.75}Pt_{0.25}$. *J. Mater. Res.* **2003**, *18*, 216−221.

(3) Presser, V.; Heon, M.; Gogotsi, Y. Carbide-Derived Carbons − From Porous Networks to Nanotubes and Graphene. *Adv. Funct. Mater.* **2011**, *21*, 810−833.

(4) Cambaz, G. Z.; Yushin, G. N.; Gogotsi, Y.; Lutsenko, V. G. Anisotropic Etching of SiC Whiskers. *Nano Lett.* **2005**, *6*, 548−551.

(5) Naguib, M.; Mochalin, V. N.; Barsoum, M. W.; Gogotsi, Y. 25th Anniversary Article: MXenes: A New Family of Two-Dimensional Materials. *Adv. Mater.* **2014**, *26*, 992−1005.

(6) Van Bommel, A. J.; Crombeen, J. E.; Van Tooren, A. LEED and Auger Electron Observations of the SiC(0001) Surface. *Surf. Sci.* **1975**, *48*, 463−472.

(7) Emtsev, K. V.; Bostwick, A.; Horn, K.; Jobst, J.; Kellogg, G. L.; Ley, L.; McChesney, J. L.; Ohta, T.; Reshanov, S. A.; Röhrl, J. Towards Wafer-Size Graphene Layers by Atmospheric Pressure Graphitization of Silicon Carbide. *Nat. Mater.* **2009**, *8*, 203−207.

(8) de Heer, W. A.; Berger, C.; Ruan, M.; Sprinkle, M.; Li, X.; Hu, Y.; Zhang, B.; Hankinson, J.; Conrad, E. Large Area and Structured Epitaxial Graphene Produced by Confinement Controlled Sublimation of Silicon Carbide. *Proc. Natl. Acad. Sci. U.S.A.* **2011**, *108*, 16900−16905.

(9) Norimatsu, W.; Kusunoki, M. Epitaxial Graphene on SiC{0001}: Advances and Perspectives. *Phys. Chem. Chem. Phys.* **2014**, *16*, 3501−3511.

(10) Novoselov, K. S.; Geim, A. K.; Morozov, S. V.; Jiang, D.; Zhang, Y.; Dubonos, S. V.; Grigorieva, I. V.; Firsov, A. A. Electric Field Effect in Atomically Thin Carbon Films. *Science* **2004**, *306*, 666−669.

(11) Berger, C.; Song, Z.; Li, T.; Li, X.; Ogbazghi, A. Y.; Feng, R.; Dai, Z.; Marchenkov, A. N.; Conrad, E. H.; First, P. N.; de Heer, W. A. Ultrathin Epitaxial Graphite: 2D Electron Gas Properties and a Route toward Graphene-based Nanoelectronics. *J. Phys. Chem. B* **2004**, *108*, 19912−19916.

(12) Varchon, F.; Mallet, P.; Magaud, L.; Veuillen, J.-Y. Rotational Disorder in Few-Layer Graphene Films on 6*H*-SiC(000-1): A Scanning Tunneling Microscopy Study. *Phys. Rev. B* **2008**, *77*, No. 165415.

(13) Cambaz, Z. G.; Yushin, G.; Osswald, S.; Mochalin, V.; Gogotsi, Y. Noncatalytic Synthesis of Carbon Nanotubes, Graphene and Graphite on SiC. *Carbon* **2008**, *46*, 841−849.

(14) Hupalo, M.; Conrad, E. H.; Tringides, M. C. Growth Mechanism for Epitaxial Graphene on Vicinal 6*H*-SiC (0001) Surfaces: A Scanning Tunneling Microscopy Study. *Phys. Rev. B* **2009**, *80*, No. 041401.

(15) Norimatsu, W.; Kusunoki, M. Transitional Structures of the Interface between Graphene and 6H−SiC (0 0 0 1). *Chem. Phys. Lett.* **2009**, *468*, 52−56.

(16) Lin, Y.-M.; Valdes-Garcia, A.; Han, S.-J.; Farmer, D. B.; Meric, I.; Sun, Y.; Wu, Y.; Dimitrakopoulos, C.; Grill, A.; Avouris, P.; Jenkins, K. A. Wafer-Scale Graphene Integrated Circuit. *Science* **2011**, *332*, 1294−1297.

(17) Lukatskaya, M. R.; Halim, J.; Dyatkin, B.; Naguib, M.; Buranova, Y. S.; Barsoum, M. W.; Gogotsi, Y. Room-Temperature Carbide-Derived Carbon Synthesis by Electrochemical Etching of MAX Phases. *Angew. Chem., Int. Ed.* **2014**, *53*, 4877−4880.

(18) Osada, M.; Sasaki, T. Exfoliated Oxide Nanosheets: New Solution to Nanoelectronics. *J. Mater. Chem.* **2009**, *19*, 2503−2511.

(19) Sugimoto, W.; Iwata, H.; Yasunaga, Y.; Murakami, Y.; Takasu, Y. Preparation of Ruthenic Acid Nanosheets and Utilization of Its Interlayer Surface for Electrochemical Energy Storage. *Angew. Chem., Int. Ed.* **2003**, *42*, 4092−4096.

(20) Rui, X.; Lu, Z.; Yu, H.; Yang, D.; Hng, H. H.; Lim, T. M.; Yan, Q. Ultrathin V_2O_5 Nanosheet Cathodes: Realizing Ultrafast Reversible Lithium Storage. *Nanoscale* **2013**, *5*, 556−560.

(21) Ma, R.; Sasaki, T. Nanosheets of Oxides and Hydroxides: Ultimate 2D Charge-Bearing Functional Crystallites. *Adv. Mater.* **2010**, *22*, 5082−5104.

DOI: 10.1021/ar500346b
Acc. Chem. Res. 2015, 48, 128−135

(22) Kalantar-zadeh, K.; Tang, J.; Wang, M.; Wang, K. L.; Shailos, A.; Galatsis, K.; Kojima, R.; Strong, V.; Lech, A.; Wlodarski, W.; Kaner, R. B. Synthesis of Nanometre-Thick MoO_3 Sheets. *Nanoscale* **2010**, *2*, 429−433.
(23) Jacobson, A. J.; Johnson, J. W.; Lewandowski, J. T. Interlayer Chemistry between Thick Transition-Metal Oxide Layers: Synthesis and Intercalation Reactions of $K[Ca_2Na_{n-3}NbnO_{3n+1}]$ $(3 \leq n \leq 7)$. *Inorg. Chem.* **1985**, *24*, 3727−3729.
(24) Gopalakrishnan, J.; Bhat, V. $A_2Ln_2Ti_3O_{10}$ (A = Potassium or Rubidium; Ln = Lanthanum or Rare Earth): A New Series of Layered Perovskites Exhibiting Ion Exchange. *Inorg. Chem.* **1987**, *26*, 4299−4301.
(25) Izawa, H.; Kikkawa, S.; Koizumi, M. Ion Exchange and Dehydration of Layered [Sodium and Potassium] Titanates, $Na_2Ti_3O_7$ and $K_2Ti_4O_9$. *J. Phys. Chem.* **1982**, *86*, 5023−5026.
(26) Sugimoto, W.; Shirata, M.; Sugahara, Y.; Kuroda, K. New Conversion Reaction of an Aurivillius Phase into the Protonated Form of the Layered Perovskite by the Selective Leaching of the Bismuth Oxide Sheet. *J. Am. Chem. Soc.* **1999**, *121*, 11601−11602.
(27) Kudo, M.; Ohkawa, H.; Sugimoto, W.; Kumada, N.; Liu, Z.; Terasaki, O.; Sugahara, Y. A Layered Tungstic Acid $H_2W_2O_7{\cdot}nH_2O$ with a Double-Octahedral Sheet Structure: Conversion Process from an Aurivillius Phase $Bi_2W_2O_9$ and Structural Characterization. *Inorg. Chem.* **2003**, *42*, 4479−4484.
(28) Omomo, Y.; Sasaki, T.; Wang; Watanabe, M. Redoxable Nanosheet Crystallites of MnO_2 Derived via Delamination of a Layered Manganese Oxide. *J. Am. Chem. Soc.* **2003**, *125*, 3568−3575.
(29) Ruiz, A. I.; Darder, M.; Aranda, P.; Jiménez, R.; Van Damme, H.; Ruiz-Hitzky, E. Bio-nanocomposites by Assembling of Gelatin and Layered Perovskite Mixed Oxides. *J. Nanosci. Nanotechnol.* **2006**, *6*, 1602−1610.
(30) Sasaki, T.; Watanabe, M.; Hashizume, H.; Yamada, H.; Nakazawa, H. Macromolecule-like Aspects for a Colloidal Suspension of an Exfoliated Titanate. Pairwise Association of Nanosheets and Dynamic Reassembling Process Initiated from It. *J. Am. Chem. Soc.* **1996**, *118*, 8329−8335.
(31) Maluangnont, T.; Matsuba, K.; Geng, F.; Ma, R.; Yamauchi, Y.; Sasaki, T. Osmotic Swelling of Layered Compounds as a Route to Producing High-Quality Two-Dimensional Materials. A Comparative Study of Tetramethylammonium versus Tetrabutylammonium Cation in a Lepidocrocite-type Titanate. *Chem. Mater.* **2013**, *25*, 3137−3146.
(32) Gogotsi, Y. G.; Andrievskiĭ, R. A. *Materials Science of Carbides, Nitrides, and Borides*; Kluwer Academic Publishers: Dordrecht, the Netherlands, 1999.
(33) Oyama, S. T. *The Chemistry of Transition Metal Carbides and Nitrides*; Springer: London, 1996.
(34) Yvon, K.; Rieger, W.; Nowotny, H. Die Kristallstruktur von V_2C. *Monatsh. Chem. Verw. Teile Anderer Wiss.* **1966**, *97*, 689−694.
(35) Naguib, M.; Kurtoglu, M.; Presser, V.; Lu, J.; Niu, J.; Heon, M.; Hultman, L.; Gogotsi, Y.; Barsoum, M. W. Two-Dimensional Nanocrystals Produced by Exfoliation of Ti_3AlC_2. *Adv. Mater.* **2011**, *23*, 4248−4253.
(36) Barsoum, M. W. *MAX Phases: Properties of Machinable Ternary Carbides and Nitrides*; John Wiley & Sons: Weinheim, Germany, 2013.
(37) Ingason, A. S.; Petruhins, A.; Dahlqvist, M.; Magnus, F.; Mockute, A.; Alling, B.; Hultman, L.; Abrikosov, I. A.; Persson, P. O. Å.; Rosen, J. A Nanolaminated Magnetic Phase: Mn_2GaC. *Mater. Res. Lett.* **2013**, *2*, 89−93.
(38) Lane, N. J.; Naguib, M.; Lu, J.; Hultman, L.; Barsoum, M. W. Structure of a New Bulk $Ti_5Al_2C_3$ MAX Phase Produced by the Topotactic Transformation of Ti_2AlC. *J. Eur. Ceram. Soc.* **2012**, *32*, 3485−3491.
(39) Novoselov, K. S.; Jiang, D.; Schedin, F.; Booth, T. J.; Khotkevich, V. V.; Morozov, S. V.; Geim, A. K. Two-Dimensional Atomic Crystals. *Proc. Natl. Acad. Sci. U.S.A.* **2005**, *102*, 10451−10453.
(40) Zhang, X.; Xu, J.; Wang, H.; Zhang, J.; Yan, H.; Pan, B.; Zhou, J.; Xie, Y. Ultrathin Nanosheets of MAX Phases with Enhanced Thermal and Mechanical Properties in Polymeric Compositions: $Ti_3Si_{0.75}Al_{0.25}C_2$. *Angew. Chem., Int. Ed.* **2013**, *52*, 4361−4365.
(41) Naguib, M.; Halim, J.; Lu, J.; Cook, K. M.; Hultman, L.; Gogotsi, Y.; Barsoum, M. W. New Two-Dimensional Niobium and Vanadium Carbides as Promising Materials for Li-ion Batteries. *J. Am. Chem. Soc.* **2013**, *135*, 15966−15969.
(42) Naguib, M.; Mashtalir, O.; Carle, J.; Presser, V.; Lu, J.; Hultman, L.; Gogotsi, Y.; Barsoum, M. W. Two-Dimensional Transition Metal Carbides. *ACS Nano* **2012**, *6*, 1322−1331.
(43) Ghidiu, M.; Naguib, M.; Shi, C.; Mashtalir, O.; Pan, L. M.; Zhang, B.; Yang, J.; Gogotsi, Y.; Billinge, S. J. L.; Barsoum, M. W. Synthesis and Characterization of Two-Dimensional Nb_4C_3 (MXene). *Chem. Commun.* **2014**, *50*, 9517−9520.
(44) Chang, F.; Li, C.; Yang, J.; Tang, H.; Xue, M. Synthesis of a New Graphene-Like Transition Metal Carbide by De-intercalating Ti_3AlC_2. *Mater. Lett.* **2013**, *109*, 295−298.
(45) Khazaei, M.; Arai, M.; Sasaki, T.; Chung, C.-Y.; Venkataramanan, N. S.; Estili, M.; Sakka, Y.; Kawazoe, Y. Novel Electronic and Magnetic Properties of Two-Dimensional Transition Metal Carbides and Nitrides. *Adv. Funct. Mater.* **2013**, *23*, 2185−2192.
(46) Khazaei, M.; Arai, M.; Sasaki, T.; Estili, M.; Sakka, Y. Two-Dimensional Molybdenum Carbides: Potential Thermoelectric Materials of the MXene Family. *Phys. Chem. Chem. Phys.* **2014**, *16*, 7841−7849.
(47) Sun, Z.; Li, S.; Ahuja, R.; Schneider, J. M. Calculated Elastic Properties of M_2AlC (M=Ti, V, Cr, Nb and Ta). *Solid State Commun.* **2004**, *129*, 589−592.
(48) Mashtalir, O.; Naguib, M.; Dyatkin, B.; Gogotsi, Y.; Barsoum, M. W. Kinetics of Aluminum Extraction from Ti_3AlC_2 in Hydrofluoric Acid. *Mater. Chem. Phys.* **2013**, *139*, 147−152.
(49) Chen, B.; Chang, F.; Yang, J.; Tang, H.; Li, C. Microstructure and Phase Transformation of Ti_3AC_2 (A = Al, Si) in Hydrofluoric Acid Solution. *Cryst. Res. Technol.* **2014**, *49*, 813−819.
(50) Halim, J.; Lukatskaya, M. R.; Cook, K. M.; Lu, J.; Smith, C. R.; Näslund, L.-Å.; May, S. J.; Hultman, L.; Gogotsi, Y.; Eklund, P.; Barsoum, M. W. Transparent Conductive Two-Dimensional Titanium Carbide Epitaxial Thin Films. *Chem. Mater.* **2014**, *26*, 2374−2381.
(51) Ghidiu, M.; Lukatskaya, M. R.; Zhao, M.-Q.; Gogotsi, Y.; Barsoum, M. W. Conductive Two-Dimensional Titanium Carbide 'Clay' with High Volumetric Capacitance. *Nature* **2014**, DOI: 10.1038/nature13970.
(52) Xie, X.; Xue, Y.; Li, L.; Chen, S.; Nie, Y.; Ding, W.; Wei, Z. Surface Al Leached Ti_3AlC_2 as a Substitute for Carbon for Use As a Catalyst Support in a Harsh Corrosive Electrochemical System. *Nanoscale* **2014**, *6*, 11035−11040.
(53) Viculis, L. M.; Mack, J. J.; Mayer, O. M.; Hahn, H. T.; Kaner, R. B. Intercalation and Exfoliation Routes to Graphite Nanoplatelets. *J. Mater. Chem.* **2005**, *15*, 974−978.
(54) Mauchamp, V.; Bugnet, M.; Bellido, E. P.; Botton, G. A.; Moreau, P.; Magne, D.; Naguib, M.; Cabioc'h, T.; Barsoum, M. W. Enhanced and Tunable Surface Plasmons in Two-Dimensional Ti_3C_2 Stacks: Electronic Structure versus Boundary Effects. *Phys. Rev. B* **2014**, *89*, No. 235428.
(55) Mashtalir, O.; Naguib, M.; Mochalin, V. N.; Dall'Agnese, Y.; Heon, M.; Barsoum, M. W.; Gogotsi, Y. Intercalation and Delamination of Layered Carbides and Carbonitrides. *Nat. Commun.* **2013**, *4*, No. 1716.
(56) Lukatskaya, M. R.; Mashtalir, O.; Ren, C. E.; Dall'Agnese, Y.; Rozier, P.; Taberna, P. L.; Naguib, M.; Simon, P.; Barsoum, M. W.; Gogotsi, Y. Cation Intercalation and High Volumetric Capacitance of Two-dimensional Titanium Carbide. *Science* **2013**, *341*, 1502−1505.
(57) Come, J.; Naguib, M.; Rozier, P.; Barsoum, M. W.; Gogotsi, Y.; Taberna, P.-L.; Morcrette, M.; Simon, P. A Non-Aqueous Asymmetric Cell with a Ti_2C-Based Two-Dimensional Negative Electrode. *J. Electrochem. Soc.* **2012**, *159*, A1368−A1373.
(58) Shi, C.; Beidaghi, M.; Naguib, M.; Mashtalir, O.; Gogotsi, Y.; Billinge, S. J. L. Structure of Nanocrystalline Ti_3C_2 MXene Using Atomic Pair Distribution Function. *Phys. Rev. Lett.* **2014**, *112*, No. 125501.
(59) Ling, Z.; Ren, C. E.; Zhao, M.; Yang, J.; Giammarco, J. M.; Qiu, J.; Barsoum, M. W.; Gogotsi, Y. Flexible and Conductive MXene Films

DOI: 10.1021/ar500346b
Acc. Chem. Res. 2015, 48, 128−135

and Nanocomposites with High Capacitance. *Proc. Natl. Acad. Sci. U.S.A.* **2014**, *111*, 16676−16681.
(60) Shein, I. R.; Ivanovskii, A. L. Graphene-like Titanium Carbides and Nitrides $Ti_{n+1}C_n$, $Ti_{n+1}N_n$ (n = 1, 2, and 3) from De-intercalated MAX Phases: First-Principles Probing of Their Structural, Electronic Properties and Relative Stability. *Comput. Mater. Sci.* **2012**, *65*, 104−114.
(61) Lane, N. J.; Barsoum, M. W.; Rondinelli, J. M. Correlation Effects and Spin-Orbit Interactions in Two-Dimensional Hexagonal 5d Transition Metal Carbides, $Ta_{n+1}C_n$ (n = 1,2,3). *Europhys. Lett.* **2013**, *101*, No. 57004.
(62) Shein, I. R.; Ivanovskii, A. L. Planar Nano-block Structures $Ti_{n+1}Al_{0.5}C_n$ and $Ti_{n+1}C_n$ (n=1, and 2) from MAX Phases: Structural, Electronic Properties and Relative Stability from First Principles Calculations. *Superlattices Microstruct.* **2012**, *52*, 147−157.
(63) Xie, Y.; Kent, P. R. C. Hybrid Density Functional Study of Structural and Electronic Properties of Functionalized $Ti_{n+1}X_n$ (X=C, N) Monolayers. *Phys. Rev. B* **2013**, *87*, No. 235441.
(64) Enyashin, A. N.; Ivanovskii, A. L. Two-Dimensional Titanium Carbonitrides and Their Hydroxylated Derivatives: Structural, Electronic Properties and Stability of MXenes $Ti_3C_{2-x}N_x(OH)_2$ from DFTB Calculations. *J. Solid State Chem.* **2013**, *207*, 42−48.
(65) Wang, S.; Li, J.-X.; Du, Y.-L.; Cui, C. First-Principles Study on Structural, Electronic and Elastic Properties of Graphene-like Hexagonal Ti_2C Monolayer. *Comput. Mater. Sci.* **2014**, *83*, 290−293.
(66) Lashgari, H.; Abolhassani, M. R.; Boochani, A.; Elahi, S. M.; Khodadadi, J. Electronic and Optical Properties of 2D Graphene-like Compounds Titanium Carbides and Nitrides: DFT Calculations. *Solid State Commun.* **2014**, *195*, 61−69.
(67) Er, D.; Li, J.; Naguib, M.; Gogotsi, Y.; Shenoy, V. B. Ti_3C_2 MXene as a High Capacity Electrode Material for Metal (Li, Na, K, Ca) Ion Batteries. *ACS Appl. Mater. Interfaces* **2014**, *6*, 11173−11179.
(68) Hu, Q.; Sun, D.; Wu, Q.; Wang, H.; Wang, L.; Liu, B.; Zhou, A.; He, J. MXene: A New Family of Promising Hydrogen Storage Medium. *J. Phys. Chem. A* **2013**, *117*, 14253−14260.
(69) Hu, Q.; Wang, H.; Wu, Q.; Ye, X.; Zhou, A.; Sun, D.; Wang, L.; Liu, B.; He, J. Two-Dimensional Sc_2C: A Reversible and High-Capacity Hydrogen Storage Material Predicted by First-Principles Calculations. *Int. J. Hydrogen Energy* **2014**, *39*, 10606−10612.
(70) Khazaei, M.; Arai, M.; Sasaki, T.; Estili, M.; Sakka, Y. The Effect of the Interlayer Element on the Exfoliation of Layered Mo_2AC (A = Al, Si, P, Ga, Ge, As or In) MAX Phases into Two-Dimensional Mo_2C Nanosheets. *Sci. Technol. Adv. Mater.* **2014**, *15*, No. 014208.
(71) Kurtoglu, M.; Naguib, M.; Gogotsi, Y.; Barsoum, M. W. First Principles Study of Two-Dimensional Early Transition Metal Carbides. *MRS Commun.* **2012**, *2*, 133−137.
(72) Lee, Y.; Cho, S. B.; Chung, Y.-C. Tunable Indirect to Direct Band Gap Transition of Monolayer Sc_2CO_2 by the Strain Effect. *ACS Appl. Mater. Interfaces* **2014**, *6*, 14724−14728.
(73) Zhao, S.; Kang, W.; Xue, J. Manipulation of Electronic and Magnetic Properties of M_2C (M = Hf, Nb, Sc, Ta, Ti, V, Zr) Monolayer by Applying Mechanical Strains. *Appl. Phys. Lett.* **2014**, *104*, No. 133106.
(74) Enyashin, A. N.; Ivanovskii, A. L. Structural and Electronic Properties and Stability of MXenes Ti_2C and Ti_3C_2 Functionalized by Methoxy Groups. *J. Phys. Chem. C* **2013**, *117*, 13637−13643.
(75) Gan, L.-Y.; Zhao, Y.-J.; Huang, D.; Schwingenschlögl, U. First-Principles Analysis of MoS_2/Ti_2C and MoS_2/Ti_2CY_2 (Y=F and OH) All-2D Semiconductor/Metal Contacts. *Phys. Rev. B* **2013**, *87*, No. 245307.
(76) Ma, Z.; Hu, Z.; Zhao, X.; Tang, Q.; Wu, D.; Zhou, Z.; Zhang, L. Tunable Band Structures of Heterostructured Bilayers with Transition-Metal Dichalcogenide and MXene Monolayer. *J. Phys. Chem. C* **2014**, *118*, 5593−5599.
(77) Tang, Q.; Zhou, Z.; Shen, P. Are MXenes Promising Anode Materials for Li Ion Batteries? Computational Studies on Electronic Properties and Li Storage Capability of Ti_3C_2 and $Ti_3C_2X_2$ (X = F, OH) Monolayer. *J. Am. Chem. Soc.* **2012**, *134*, 16909−16916.
(78) Xie, Y.; Dall'Agnese, Y.; Naguib, M.; Gogotsi, Y.; Barsoum, M. W.; Zhuang, H. L.; Kent, P. R. C. Prediction and Characterization of MXene Nanosheet Anodes for Non-Lithium-Ion Batteries. *ACS Nano* **2014**, *8*, 9606−9615.
(79) Xie, Y.; Naguib, M.; Mochalin, V. N.; Barsoum, M. W.; Gogotsi, Y.; Yu, X.; Nam, K.-W.; Yang, X.-Q.; Kolesnikov, A. I.; Kent, P. R. C. Role of Surface Structure on Li-Ion Energy Storage Capacity of Two-Dimensional Transition-Metal Carbides. *J. Am. Chem. Soc.* **2014**, *136*, 6385−6394.
(80) Zhao, S.; Kang, W.; Xue, J. Role of Strain and Concentration on the Li Adsorption and Diffusion Properties on Ti_2C Layer. *J. Phys. Chem. C* **2014**, *118*, 14983−14990.
(81) Naguib, M.; Come, J.; Dyatkin, B.; Presser, V.; Taberna, P.-L.; Simon, P.; Barsoum, M. W.; Gogotsi, Y. MXene: A Promising Transition Metal Carbide Anode for Lithium-Ion Batteries. *Electrochem. Commun.* **2012**, *16*, 61−64.
(82) Levi, M. D.; Lukatskaya, M. R.; Sigalov, S.; Beidaghi, M.; Shpigel, N.; Daikhin, L.; Aurbach, D.; Barsoum, M. W.; Gogotsi, Y. Solving the Capacitive Paradox of 2D MXene using Electrochemical Quartz-Crystal Admittance and In Situ Electronic Conductance Measurements. *Adv. Energy Mater.* **2014**, DOI: 10.1002/aenm.201400815.
(83) Dall'Agnese, Y.; Lukatskaya, M. R.; Cook, K. M.; Taberna, P.-L.; Gogotsi, Y.; Simon, P. High Capacitance of Surface-Modified 2D Titanium Carbide in Acidic Electrolyte. *Electrochem. Commun.* **2014**, *48*, 118−122.
(84) Li, X.; Fan, G.; Zeng, C. Synthesis of Ruthenium Nanoparticles Deposited on Graphene-Like Transition Metal Carbide As an Effective Catalyst for the Hydrolysis of Sodium Borohydride. *Int. J. Hydrogen Energy* **2014**, *39*, 14927−14934.
(85) Gao, Y.; Wang, L.; Li, Z.; Zhou, A.; Hu, Q.; Cao, X. Preparation of MXene-Cu_2O Nanocomposite and Effect on Thermal Decomposition of Ammonium Perchlorate. *Solid State Sci.* **2014**, *35*, 62−65.
(86) Xie, X.; Chen, S.; Ding, W.; Nie, Y.; Wei, Z. An Extraordinarily Stable Catalyst: Pt NPs Supported on Two-Dimensional $Ti_3C_2X_2$ (X = OH, F) Nanosheets for Oxygen Reduction Reaction. *Chem. Commun.* **2013**, *49*, 10112−10114.
(87) Peng, Q.; Guo, J.; Zhang, Q.; Xiang, J.; Liu, B.; Zhou, A.; Liu, R.; Tian, Y. Unique Lead Adsorption Behavior of Activated Hydroxyl Group in Two-Dimensional Titanium Carbide. *J. Am. Chem. Soc.* **2014**, *136*, 4113−4116.
(88) Naguib, M.; Mashtalir, O.; Lukatskaya, M. R.; Dyatkin, B.; Zhang, C.; Presser, V.; Gogotsi, Y.; Barsoum, M. W. One-Step Synthesis of Nanocrystalline Transition Metal Oxides on Thin Sheets of Disordered Graphitic Carbon by Oxidation of MXenes. *Chem. Commun.* **2014**, *50*, 7420−7423.
(89) Bauer, E.; Rogl, G.; Chen, X.-Q.; Khan, R. T.; Michor, H.; Hilscher, G.; Royanian, E.; Kumagai, K.; Li, D. Z.; Li, Y. Y.; Podloucky, R.; Rogl, P. Unconventional Superconducting Phase in the Weakly Correlated Noncentrosymmetric Mo_3Al_2C Compound. *Phys. Rev. B* **2010**, *82*, No. 064511.

DOI: 10.1021/ar500346b
Acc. Chem. Res. 2015, 48, 128−135